

Algorithm to calculate off-plane magnetic field from an on-plane field map

N. Tsoupas

May 2018

Collider Accelerator Department
Brookhaven National Laboratory

U.S. Department of Energy
USDOE Office of Science (SC), Nuclear Physics (NP) (SC-26)

Notice: This technical note has been authored by employees of Brookhaven Science Associates, LLC under Contract No. DE-SC0012704 with the U.S. Department of Energy. The publisher by accepting the technical note for publication acknowledges that the United States Government retains a non-exclusive, paid-up, irrevocable, world-wide license to publish or reproduce the published form of this technical note, or allow others to do so, for United States Government purposes.

DISCLAIMER

This report was prepared as an account of work sponsored by an agency of the United States Government. Neither the United States Government nor any agency thereof, nor any of their employees, nor any of their contractors, subcontractors, or their employees, makes any warranty, express or implied, or assumes any legal liability or responsibility for the accuracy, completeness, or any third party's use or the results of such use of any information, apparatus, product, or process disclosed, or represents that its use would not infringe privately owned rights. Reference herein to any specific commercial product, process, or service by trade name, trademark, manufacturer, or otherwise, does not necessarily constitute or imply its endorsement, recommendation, or favoring by the United States Government or any agency thereof or its contractors or subcontractors. The views and opinions of authors expressed herein do not necessarily state or reflect those of the United States Government or any agency thereof.

ALGORITHM TO CALCULATE OFF-PLANE MAGNETIC FIELD FROM AN ON-PLANE FIELD MAP *

N. Tsoupas[†], J. S. Berg, S. Brooks, F. Méot, V. Ptitsyn, D. Trbojevic

Brookhaven National Laboratory, Upton, NY, USA

S. Machida

STFC Rutherford Appleton Laboratory England

Abstract

An algorithm is presented to calculate the field components $[B_x(x, y, z), B_y(x, y, z), B_z(x, y, z)]$ of the magnetic field at a point (x, y, z) in space, from the knowledge of the components $[B_x(x, y = 0, z), B_y(x, y = 0, z), B_z(x, y = 0, z)]$ on a "reference plane", which is normal to the y -axis at $y=0$. The algorithm, which is a general one and is not restricted to fields with mid-plane symmetry is based on the Taylor series expansion of the magnetic field components at any point in space in terms of the distance (y) of the point from the reference plane. The coefficients of the Taylor series expansion are expressed in terms of the on-plane field components and their partial derivatives with respect to spatial coordinates (x, z) . The field components are usually generated from magnetic field measurements on a rectangular grid on the plane. The required partial derivatives of the field components on the plane can be computed with two methods; numerically, or by fitting a polynomial function to the experimentally measured values of the field components and subsequently take the required partial derivatives of the polynomial function. Each of these two method which calculates the partial derivatives of the field components on the plane, is applied to calculate the off-plane field components of the magnetic field generated by a modified Halbach magnet [1] of inner radius of 4.4 cm and it is found that each method provides accurate results with a relative error $<1\%$ deviation from the "ideal" fields if the y distance of the point from the reference plane is smaller than 2 cm. This algorithm is part of the RAYTRACE computer code [2] and has been applied [3] on a dipole magnet with median plane symmetry.

INTRODUCTION

With the advent of the technology to perform more accurate magnetic field measurements on magnets which guide and focus charged particle beams, the beam optics calculations very often rely on magnetic field measurements of a single or many magnets of a beam line system. These measurements are performed on a 3D or 2D rectangular grid in space. If the measurements of the magnetic fields are made on a 3D rectangular grid this field map is used directly in computer codes [2,4] which integrate the equation of motion of a charged particle in this 3D field map to derive the optical properties of the system. However if the magnetic field measurements are made on a plane grid, the Maxwell equations must be used to calculate, from the measured components of the magnetic field on a plane grid, the field components at any point in space. Similar algorithms which calculate 3D fields at a point in space from 2D field maps on a surface are being used by the computer code zgoubi [5, 6]. Other algorithms which calculate B-fields in space from the knowledge of the field along the symmetry axis of an axisymmetric magnet have been developed and are used in computer codes [2]. A recent paper on such an algorithm appears in ref. [7]. In this technical note an algorithm is presented which calculates the magnetic field at any given point in space from the knowledge of the magnetic field components on a plane which in this paper is referred as the reference plane. Fig. 1 shows the grid points (intersection points of the red lines) on a plane where the magnetic field components (yellow arrows) are measured experimentally. The task is to calculate the field components (blue arrows) at any given point in space, at a distance y from the plane, from the knowledge of the field components on the reference plane. No magnetic material exists in between the plane and the point in space where the field is calculated. The algorithm provides the values of the components of the magnetic field at a distance y from the plane. Although most of the magnets used in the applications of charged particle beam optics and in particle accelerators have median plane symmetry, in this technical note we will remove this constrain of median plane symmetry, and the only requirement will be the experimentally measure field components of the magnetic field at the grid points of the plane. The algorithm is based on the Taylor series expansion of the magnetic field components at the point of interest in terms of the y coordinate which is the distance from the plane of the point at which the field is to be calculated. The coefficients of the Taylor series expansion are expressed in terms of the field components at the grid points on the reference plane and their spatial partial derivatives with respect to x and z on the plane.

* Work supported by the US Department of Energy

[†] tsoupas@bnl.gov

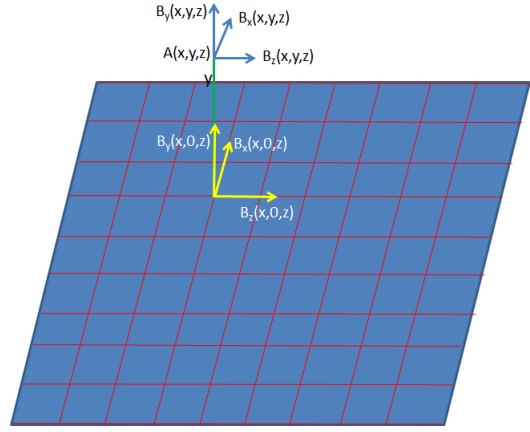


Figure 1: A schematic diagram of a grid on a plane. The magnetic field components (yellow arrows) at any grid point on the plane are measured. The algorithm calculates the magnetic field components (blue arrows) at any given point in space at a distance y from the plane. In this paper this plane is referred as the reference plane.

THE DEVELOPMENT OF THE ALGORITHM

In this section we present in details the development of the algorithm which calculates the off plane components $[B_x(x, y, z), B_y(x, y, z), B_z(x, y, z)]$ of the magnetic field at a particular point $A(x,y,z)$ of a magnet and at a distance y from the plane over which the field components, on specified grid points like the intersection of the red lines in Fig. 1, are known. We start by expanding the components of the field $\vec{B}(x, y, z)$ as a Maclaurin series in y to 4th order.

$$B_i(x, y, z) = B_i(x, 0, z) + \sum_{j=1}^4 a_{ij}(x, z)y^j \quad (1)$$

The index i runs from 1 to 3 with $(1,2,3) \Leftrightarrow (x, y, z)$ and the index j in this expansion runs from 1 to 4. Since the values of the field components on the plane ($y=0$) are known the task is to express the coefficients of expansion $a_{ij}(x, z)$ in terms of these field components on the plane and also in terms of their partial derivatives of these field components with respect to the x and z spatial coordinates. By applying the Maxwell's equation $\vec{\nabla} \cdot \vec{B}(x, y, z) = 0$ on the magnetic field given by the Taylor series expansion in Eq.1 the following relation is obtained.

$$\begin{aligned} \vec{\nabla} \cdot \vec{B}(x, y, z) &= \frac{\partial B_x(x, 0, z)}{\partial x} + \sum_{j=1}^4 \frac{\partial a_{xj}(x, z)}{\partial x} y^j + \\ &\quad \frac{\partial B_y(x, 0, z)}{\partial y} + \sum_{j=1}^4 j a_{yj}(x, z) y^{j-1} + \\ &\quad \frac{\partial B_z(x, 0, z)}{\partial z} + \sum_{j=1}^4 \frac{\partial a_{zj}(x, z)}{\partial z} y^j = 0 \end{aligned} \quad (2)$$

In this paper is assumed that all partial derivatives of the measured magnetic fields on the plane with respect to y are equal to zero since the measured fields on the plane do not explicitly depend on y . Zeroing the coefficients of the powers of y in Eq. (2) is obtained:

$$a_{y1}(x, z) = - \left(\frac{\partial B_x(x, 0, z)}{\partial x} + \frac{\partial B_z(x, 0, z)}{\partial z} \right) \quad (3)$$

$$\frac{\partial a_{xj}(x, z)}{\partial x} + (j+1)a_{y(j+1)}(x, z) + \frac{\partial a_{zj}(x, z)}{\partial z} = 0 \quad \text{for } j = 1 \text{ to } 3 \quad (4)$$

Use of the Maxwell's equation $\vec{\nabla} \times \vec{B}(x, y, z) = 0$ yields:

$$\vec{\nabla} \times \vec{B}(x, y, z) = \left(\frac{\partial B_z}{\partial y} - \frac{\partial B_y}{\partial z} \right) \hat{i} + \left(\frac{\partial B_x}{\partial z} - \frac{\partial B_z}{\partial x} \right) \hat{j} + \left(\frac{\partial B_y}{\partial x} - \frac{\partial B_x}{\partial y} \right) \hat{k} = 0 \quad (5)$$

Substituting Eq. (1) in the x -component of Eq. (5) is obtained:

$$\frac{\partial B_z(x, 0, z)}{\partial y} + a_{z1} + 2a_{z2}y + 3a_{z3}y^2 + 4a_{z4}y^3 = \frac{\partial B_y(x, 0, z)}{\partial z} + \frac{\partial a_{y1}}{\partial z}y + \frac{\partial a_{y2}}{\partial z}y^2 + \frac{\partial a_{y3}}{\partial z}y^3 + \frac{\partial a_{y4}}{\partial z}y^4 \quad (6)$$

Zeroing the coefficients of the powers of y in Eq. (6) is obtained:

$$a_{z1} = \frac{\partial B_y(x, 0, z)}{\partial z} \quad (7)$$

$$(j+1)a_{zj} = \frac{\partial a_{yj}(x, z)}{\partial z} \quad \text{for } j = 1 \text{ to } 3 \quad (8)$$

Setting the z -component of Eq. (5) to zero the relations below are obtained:

$$a_{x1} = \frac{\partial B_y(x, 0, z)}{\partial x} \quad (9)$$

$$(j+1)a_{xj} = \frac{\partial a_{yj}(x, z)}{\partial x} \quad \text{for } j = 1 \text{ to } 3 \quad (10)$$

Expression of the coefficients a_{ij} in terms of known Quantities

Using the results of the previous subsection the coefficients a_{ij} are expressed in terms of the derivatives of the B-fields on the plane.

The 1st order a_{i1} coefficients

From Eqs. (9, 3, and 7)

$$a_{x1} = \frac{\partial B_y(x, 0, z)}{\partial x} \quad (11)$$

$$a_{y1}(x, z) = -\left(\frac{\partial B_x(x, 0, z)}{\partial x} + \frac{\partial B_z(x, 0, z)}{\partial z}\right) \quad (12)$$

$$a_{z1} = \frac{\partial B_y(x, 0, z)}{\partial z} \quad (13)$$

The 2nd order a_{i2} coefficients

From Eq. (10, 4, 8, and 11, 12, 13)

$$a_{x2} = -\frac{1}{2}\left(\frac{\partial^2 B_x(x, 0, z)}{\partial x^2} + \frac{\partial^2 B_z(x, 0, z)}{\partial x \partial z}\right) \quad (14)$$

$$a_{y2} = -\frac{1}{2}\left(\frac{\partial^2 B_y(x, 0, z)}{\partial x^2} + \frac{\partial^2 B_y(x, 0, z)}{\partial z^2}\right) \quad (15)$$

$$a_{z2} = -\frac{1}{2}\left(\frac{\partial^2 B_x(x, 0, z)}{\partial z \partial x} + \frac{\partial^2 B_z(x, 0, z)}{\partial z^2}\right) \quad (16)$$

The 3rd order a_{i3} coefficients

From Eq. (10, 4, 8, and 14, 15, 16)

$$a_{x3} = -\frac{1}{6}\left(\frac{\partial^3 B_y(x, 0, z)}{\partial x^3} + \frac{\partial^3 B_y(x, 0, z)}{\partial x \partial z^2}\right) \quad (17)$$

$$a_{y3} = \frac{1}{6}\left(\frac{\partial^3 B_x(x, 0, z)}{\partial x^3} + \frac{\partial^3 B_z(x, 0, z)}{\partial x^2 \partial z} + \frac{\partial^3 B_x(x, 0, z)}{\partial z^2 \partial x} + \frac{\partial^3 B_z(x, 0, z)}{\partial z^3}\right) \quad (18)$$

$$a_{z3} = -\frac{1}{6}\left(\frac{\partial^3 B_y(x, 0, z)}{\partial z \partial x^2} + \frac{\partial^3 B_y(x, 0, z)}{\partial z^3}\right) \quad (19)$$

The 4th order a_{i4} coefficients

From Eq. (10, 4, 8, and and 17, 18, 19)

$$a_{x4} = \frac{1}{24} \left(\frac{\partial^4 B_x(x, 0, z)}{\partial x^4} + \frac{\partial^4 B_z(x, 0, z)}{\partial x^3 \partial z} + \frac{\partial^4 B_x(x, 0, z)}{\partial x^2 \partial z^2} + \frac{\partial^4 B_z(x, 0, z)}{\partial x \partial z^3} \right) \quad (20)$$

From Eq. (6) (25) and (27)

$$a_{y4} = -\frac{1}{24} \left(\frac{\partial^4 B_y(x, 0, z)}{\partial x^4} + 2 \frac{\partial^4 B_y(x, 0, z)}{\partial x^2 \partial z^2} + \frac{\partial^4 B_y(x, 0, z)}{\partial z^4} \right) \quad (21)$$

From Eq. (13) and (26)

$$a_{z4} = \frac{1}{24} \left(\frac{\partial^4 B_x(x, 0, z)}{\partial z \partial x^3} + \frac{\partial^4 B_z(x, 0, z)}{\partial x^2 \partial z^2} + \frac{\partial^4 B_x(x, 0, z)}{\partial z^3 \partial x} + \frac{\partial^4 B_z(x, 0, z)}{\partial z^4} \right) \quad (22)$$

CALCULATION OF THE DERIVATIVES

In the previous section the coefficients a_{ij} in Eq. 1 are expressed as a function of the field components on the reference plane, and as a function of their partial derivatives of these field components with respect to the x and y coordinates. The numerical values of the three components of the field on a plane are usually provided as the values of these components at specified points on a rectangular grid of the reference plane. In the RAYTRACE code [2] two methods are used to calculate the derivatives of the fields on the plane; the "fit of a function" method' and the "numerical" method'. Both methods are described in the following two sub sections. The numerical comparison of the two methods, each applied to calculate the magnetic field at a point (x, y, z) is described in one of the following sections.

Fit a Function method

Fig. 2 shows the grid points of the global (x, z) coordinate system where the field components $[B_x(x, y = 0, z), B_y(x, y = 0, z), B_z(x, y = 0, z)]$ are measured, and also shows two of the many "small-grid-areas" (ABCD), (EFGH) in which the global grid is partitioned. The small grid areas may partially overlap with each other, and each area can be characterized

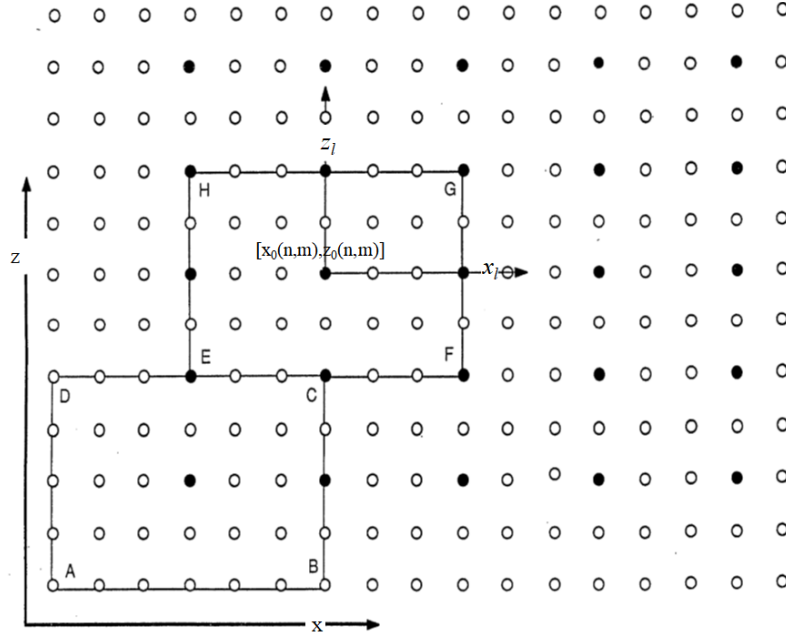


Figure 2: The large 2D grid in the (x, z) coordinate system is partitioned in many "small-grid-areas" two of these small areas (ABCD), (EFGH) are shown. The small grid areas may overlap, and each area can be characterized by the (n, m) indices and its local (x_l, y_l) coordinate system. The local coordinates (x_l, y_l) of each small grid are related to the global (x, z) coordinates through the equations $x = x_0(n, m) + x_l$ and $z = z_0(n, m) + z_l$

by the (n, m) indices and its associated (x_l, y_l) local coordinate system. With this method a polynomial function shown in Eq. 23, is fitted to the experimentally measured values of the magnetic field components. The local coordinates (x_l, y_l) of each small grid are related to the global coordinates (x, z) through the equations $x = x_0(n, m) + x_l$ and $z = z_0(n, m) + z_l$, where

$x_0(n, m)$ and $z_0(n, m)$ are the global coordinates of the centers $(x_l, y_l)=(0,0)$ of the "small-grid-area" which is characterized by the indices (n, m) .

$$B_i(n, m, x_l, z_l) = B_i(n, m, 0, 0) + \sum_{j=1}^4 \sum_{k=1}^4 c_{i,n,m,j,k} (x_l)^j (z_l)^k \quad (23)$$

In Eq. 23 the index i corresponds to the field component with $i=(1,2,3) \Leftrightarrow (x, y, z)$ and the indices n, m correspond to the particular "small-grid-area" of the global grid. The x_l, z_l variables are the local coordinates of this "small-grid-area" which are related to the global coordinates (x, z) through equations mentioned earlier. The coefficients $c_{i,n,m,j,k}$ are calculated using the method of Singular Value Decomposition (SVD) [9] which is applied to solve N equations with M unknowns ($N \geq M$). This method of fitting a function to the experimentally measured field components at the grid points of a rectangular grid on the median plane of a magnet has been used in the RAYTRACE code to calculate the beam optics of the AGS synchrotron [8] using the median plane field maps of the AGS combined function magnets. An example of the application of this method will be given in one of the following sections.

Numerical method

The numerical method is based in generating a local grid as shown in Fig. 3. The field component $B_i(x, z)$ at any grid point of Fig. 3 can be expressed with the following equation (24) which is the 2D Maclaurin series expansion of the field component in terms of the local coordinates $\Delta x_l, \Delta z_l$.

$$B_i(x, z) = \sum_{j=0}^3 \sum_{k=0}^3 \frac{k!}{j!(j-k)!} \frac{\partial^j B_i(x, z) \partial^{j-k} B_i(x, z)}{\partial x^j \partial z^{j-k}} (\Delta x_l)^j (\Delta z_l)^{j-k} \quad (24)$$

Substituting in Eq. 24 the field values of each component $B_i(x, z)$ corresponding to the grid points of Fig. 3 one can

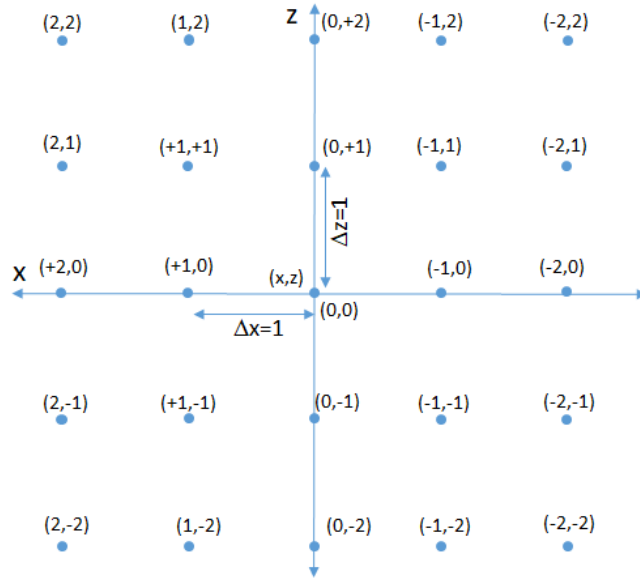


Figure 3: The field components $[B_x(x, y = 0, z), B_y(x, y = 0, z), B_z(x, y = 0, z)]$ on each grid points must be known for the calculation of the field derivatives by using the equation (24).

generate enough equations sufficient to calculate the numerical values of the required derivatives for the calculation of the coefficients a_{ij} .

As an example of calculating the derivatives appearing in the one-column of the matrix equation of Fig. 4, the values of the field components $B_i(i_x, i_z)$ appearing in the last one-column matrix were selected from the grid points (i_x, i_z) . This set of N linear equations with N unknowns can be solved by "hand" or much easier using the "mathematica" computer code. In the following subsection are the expressions of the required partial derivatives of the field components, in terms of on-the-plane field components $B_i(i_x, i_z)$. These derivatives are required for the calculation of the coefficients a_{ij} .

$$\begin{pmatrix}
1 & 0 & 0 & 0 & 0 & 0 & 0 & 0 & 0 & 0 & 0 & 0 & 0 \\
1 & 1 & 0 & 1/2 & 0 & 0 & 1/6 & 0 & 0 & 0 & 1/24 & 0 & 0 \\
1 & -1 & 0 & 1/2 & 0 & 0 & -1/6 & 0 & 0 & 0 & 1/24 & 0 & 0 \\
1 & 0 & 1 & 0 & 0 & 1/2 & 0 & 0 & 0 & 1/6 & 0 & 0 & 1/24 \\
1 & 0 & -1 & 0 & 0 & 1/2 & 0 & 0 & 0 & -1/6 & 0 & 0 & 1/24 \\
1 & 2 & 0 & 2 & 0 & 0 & 4/3 & 0 & 0 & 0 & 2/3 & 0 & 0 \\
1 & -2 & 0 & 2 & 0 & 0 & -4/3 & 0 & 0 & 0 & 2/3 & 0 & 0 \\
1 & 0 & 2 & 0 & 0 & 2 & 0 & 0 & 0 & 4/3 & 0 & 0 & 2/3 \\
1 & 0 & -2 & 0 & 0 & 2 & 0 & 0 & 0 & -4/3 & 0 & 0 & 2/3 \\
1 & 1 & 1 & 1/2 & 1 & 1/2 & 1/6 & 1/2 & 1/2 & 1/6 & 1/24 & 1/4 & 1/24 \\
1 & -1 & -1 & 1/2 & 1 & 1/2 & -1/6 & -1/2 & -1/2 & -1/6 & 1/24 & 1/4 & 1/24 \\
1 & -1 & 1 & 1/2 & -1 & 1/2 & -1/6 & 1/2 & -1/2 & 1/6 & 1/24 & 1/4 & 1/24 \\
1 & 1 & -1 & 1/2 & -1 & 1/2 & 1/6 & -1/2 & 1/2 & -1/6 & 1/24 & 1/4 & 1/24
\end{pmatrix}
\begin{pmatrix}
B_0 \\
\partial/\partial x \\
\partial/\partial y \\
\partial^2/\partial x^2 \\
\partial^2/\partial x\partial z \\
\partial^2/\partial z^2 \\
\partial^3/\partial x^3 \\
\partial^3/\partial x^2\partial z \\
\partial^3/\partial x\partial z^2 \\
\partial^3/\partial z^3 \\
\partial^4/\partial x^4 \\
\partial^4/\partial x^2\partial z^2 \\
\partial^4/\partial z^4
\end{pmatrix}
=
\begin{pmatrix}
B_i(0,0) \\
B_i(+1,0) \\
B_i(-1,0) \\
B_i(0,+1) \\
B_i(0,-1) \\
B_i(+2,0) \\
B_i(-2,0) \\
B_i(0,+2) \\
B_i(0,-2) \\
B_i(+1,+1) \\
B_i(-1,-1) \\
B_i(1,-1) \\
B_i(-1,+1)
\end{pmatrix}$$

Figure 4: A set of N linear equations with N unknowns in a matrix form $A \cdot X = B$ to calculate the partial derivatives appearing in the (one-column N-rows) matrix.

First order derivatives

$$\begin{aligned}
\frac{\partial B_i(x,z)}{\partial x} &= \frac{1}{12\Delta x} \{8[B_i(1,0) - B_i(-1,0)] - [B_i(2,0) - B_i(-2,0)]\} \quad (i = x, y, z) \\
\frac{\partial B_i(x,z)}{\partial z} &= \frac{1}{12\Delta z} \{8[B_i(0,1) - B_i(0,-1)] - [B_i(0,2) - B_i(0,-2)]\} \quad (i = x, y, z)
\end{aligned}$$

Second order derivatives

$$\begin{aligned}
\frac{\partial^2 B_i(x,z)}{\partial x^2} &= \frac{1}{12(\Delta x)^2} \{16[B_i(1,0) - B_i(-1,0)] - [B_i(2,0) - B_i(-2,0)] - 30B(0,0)\} \quad (i = x, y, z) \\
\frac{\partial^2 B_i(x,z)}{\partial z^2} &= \frac{1}{12(\Delta z)^2} \{16[B_i(0,1) - B_i(0,-1)] - [B_i(0,2) - B_i(0,-2)] - 30B(0,0)\} \quad (i = x, y, z)
\end{aligned}$$

The second order derivatives below have been calculated in three different ways depending on the grid points selected from Fig. 3 to generate the set of N equations with N unknowns in Fig. 4 which calculates the derivatives. The numerical values of the three derivatives bellow differs by less than 0.04%. This difference is much smaller than the calculated error of the derivatives when the derivatives are calculated from experimental field measurements therefore any of the three expressions can be used in the calculations of the field $\vec{B}(x, y, z)$.

$$\begin{aligned}
\frac{\partial^2 B_i(x,z)}{\partial x \partial z} &= \frac{1}{4(\Delta x)\Delta z} \{[B_i(1,1) - B_i(-1,-1)] - [B_i(1,-1) - B_i(-1,1)]\} \quad (i = x, y, z) \\
\frac{\partial^2 B_i(x,z)}{\partial x \partial z} &= \frac{1}{4(\Delta x)\Delta z} \{4 * B_i(0,0) + 3[B_i(1,1) + B_i(-1,-1)] - (\frac{1}{3})[B_i(1,-1) + B_i(-1,1)] \\
&- (\frac{1}{3})[B_i(2,1) + B_i(-2,-1)] - (\frac{1}{3})[B_i(1,2) + B_i(-1,-2)] - (\frac{7}{3})[B_i(1,0) + B_i(-1,0)] \\
&- (\frac{7}{3})[B_i(0,1) + B_i(0,-1)] + (\frac{1}{3})[B_i(2,0) + B_i(-2,0)] + (\frac{1}{3})[B_i(0,2) + B_i(0,-2)]\} \quad (i = x, y, z) \\
\frac{\partial^2 B_i(x,z)}{\partial x \partial z} &= \frac{1}{12(\Delta x)\Delta z} \{12 * B_i(0,0) - [B_i(1,2) + B_i(-1,-2)] - [B_i(2,1) + B_i(-2,-1)] \\
&+ 9[B_i(1,1) + B_i(-1,-1)] - 7[B_i(1,0) + B_i(-1,0)] - 7[B_i(0,1) + B_i(0,-1)] \\
&- [B_i(1,-1) + B_i(-1,1)] + [B_i(2,0) + B_i(-2,0)] + [B_i(0,2) + B_i(0,-2)]\} \quad (i = x, y, z)
\end{aligned}$$

Third order derivatives

$$\begin{aligned}
\frac{\partial^3 B_i(x,z)}{\partial x^3} &= \frac{1}{2(\Delta x)^3} \{[B_i(2,0) - B_i(-2,0)] - 2[B_i(1,0) - B_i(-1,0)]\} \quad (i = x, y, z) \\
\frac{\partial^3 B_i(x,z)}{\partial z^3} &= \frac{1}{2(\Delta z)^3} \{[B_i(0,2) - B_i(0,-2)] - 2[B_i(0,1) - B_i(0,-1)]\} \quad (i = x, y, z) \\
\frac{\partial^3 B_i(x,z)}{\partial x^2 \partial z} &= \frac{1}{2(\Delta x)^2 \Delta z} \{[B_i(1,1) - B_i(-1,-1)] - [B_i(1,-1) - B_i(-1,1)] - 2[B_i(0,1) - B_i(0,-1)]\} \quad (i = x, y, z) \\
\frac{\partial^3 B_i(x,z)}{\partial x \partial z^2} &= \frac{1}{2(\Delta x) (\Delta z)^2} \{[B_i(1,1) - B_i(-1,-1)] + [B_i(1,-1) - B_i(-1,1)] - 2[B_i(1,0) - B_i(-1,0)]\} \quad (i = x, y, z)
\end{aligned}$$

Fourth order derivatives

$$\begin{aligned}\frac{\partial^4 B_i(x,z)}{\partial x^4} &= \frac{1}{(\Delta x)^4} \{ [B_i(2,0) + B_i(-2,0)] - 4[B_i(1,0) + B_i(-1,0)] + 6B_i(0,0) \} \quad (i = x, y, z) \\ \frac{\partial^4 B_i(x,z)}{\partial z^4} &= \frac{1}{(\Delta z)^4} \{ [B_i(0,2) + B_i(0,-2)] - 4[B_i(0,1) + B_i(0,-1)] + 6B_i(0,0) \} \quad (i = x, y, z) \\ \frac{\partial^4 B_i(x,z)}{\partial x^3 \partial z} &= \frac{1}{2(\Delta x)^3(\Delta z)} \{ [B_i(2,1) + B_i(-2,-1)] - [B_i(2,0) + B_i(-2,0)] - 3[B_i(1,1) + B_i(-1,-1)] \\ &\quad - [B_i(1,-1) + B_i(-1,1)] + 4[B_i(1,0) + B_i(-1,0)] + 3[B_i(0,1) + B_i(0,-1)] - 6B_i(0,0) \} \quad (i = x, y, z) \\ \frac{\partial^4 B_i(x,z)}{\partial x^2 \partial z^2} &= \frac{1}{(\Delta x)^2(\Delta z)^2} \{ [B_i(1,1) - B_i(-1,-1)] + [B_i(1,-1) - B_i(-1,1)] - 2[B_i(1,0) - B_i(-1,0)] \\ &\quad - 2[B_i(0,1) - B_i(0,-1)] - 4B_i(0,0) \} \quad (i = x, y, z) \\ \frac{\partial^4 B_i(x,z)}{\partial x \partial z^3} &= \frac{1}{2(\Delta x)(\Delta z)^3} \{ [B_i(1,2) + B_i(-1,-2)] - [B_i(0,2) + B_i(0,-2)] - 3[B_i(1,1) + B_i(-1,-1)] \\ &\quad - [B_i(1,-1) + B_i(-1,1)] + 4[B_i(0,1) + B_i(0,-1)] + 3[B_i(1,0) + B_i(-1,0)] - 6B_i(0,0) \} \quad (i = x, y, z)\end{aligned}$$

COMPARISON OF THE "fit a function method" WITH THE "numerical method" MEDIAN PLANE SYMMETRY

This section is devoted to the comparison of the "fit a function method" with that of the "numerical method" that both were discussed earlier. The comparison consist in computing the components $[B_x(x, y_{const}, z), B_y(x, y_{const}, z), B_z(x, y_{const}, z)]$ of the B-field of a magnet on a plane at a distance y_{const} from the reference plane ($y=0$), using each of the methods, and comparing each set of these fields components against the "exact fields" which were calculated by the 3D OPERA computer code [11]. Fig. 5 is an isometric view of one of the cell's magnets of the CBETA accelerator [1] whose field components are calculated by the 3D OPERA code, and are used for the comparison of the two methods.

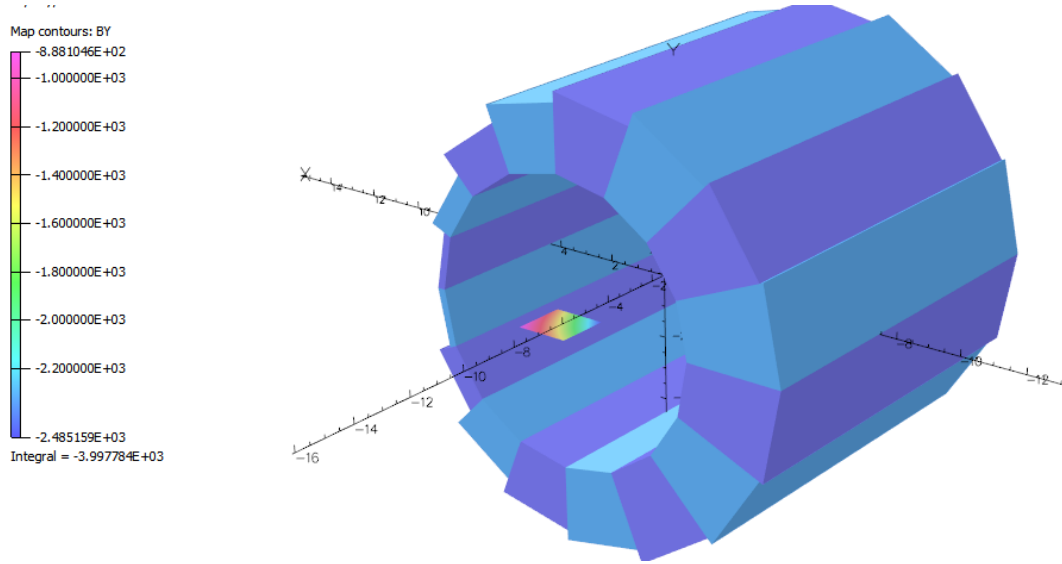


Figure 5: An isometric view of a modified Halbach magnet which generates a combined dipole and quadrupole field. The fields of this magnet are used in testing the two methods as it is described in this section.

The procedure of comparison of the fields as calculated by each of the two methods is described below.

1. The exact field components $[B_x(x, y, z), B_y(x, y, z), B_z(x, y, z)]$ over the space generated by the magnet shown in Fig. 5 have been calculated using the OPERA computer code. This magnet is a modified Halbach magnet and is designed to provide a dipole and a quadrupole field. These OPERA-calculated-fields are considered to be the "exact fields" and will be used as the basis of comparison with the fields calculated by the "fit a function method" and the "numerical method".
2. A rectangular area $16 \times 16 \text{ mm}^2$ normal to the y axis located on the median plane and centered on a vertical plane which is in conduct with one of the hard edges of the magnet, is chosen, and the field components $[B_x(x, y = 0, z), B_y(x, y = 0, z), B_z(x, y = 0, z)]$ are tabulated at every grid point of the area. The grid size over the area is

1 mm in either x or z direction. The field components $[B_x(x, y = 0, z), B_y(x, y = 0, z), B_z(x, y = 0, z)]$ at each of the grid points of the $16 \times 16 \text{ mm}^2$ area have been calculated by the OPERA computer code and the color contours of the B_y field component are plotted over the area. These field components over this area may be considered that they correspond to the experimentally measured field components of the magnet. A histogram plot of the $B_y(x, y = 0, z)$ field component over this $16 \times 16 \text{ mm}^2$ rectangular area is shown in Fig. 6. The algorithm uses the field components at the grid points shown over the rectangular area. The (0,0) point shown in Fig. 6 is the origin of the local coordinate system (x_l, y_l) for this particular "small grid area".

3. In this step the algorithm is applied to calculate the $[B_x(x, y_{const}, z), B_y(x, y_{const}, z), B_z(x, y_{const}, z)]$ field components, at a plane parallel to the $y=0$ plane and located at a distance y_{const} from the reference plane ($y=0$), using the "fit a function method" or the "numerical method".

4. Each set of the calculated field components on this plane are compared with the "exact field components" as calculated by the OPERA computer code on the same plane.

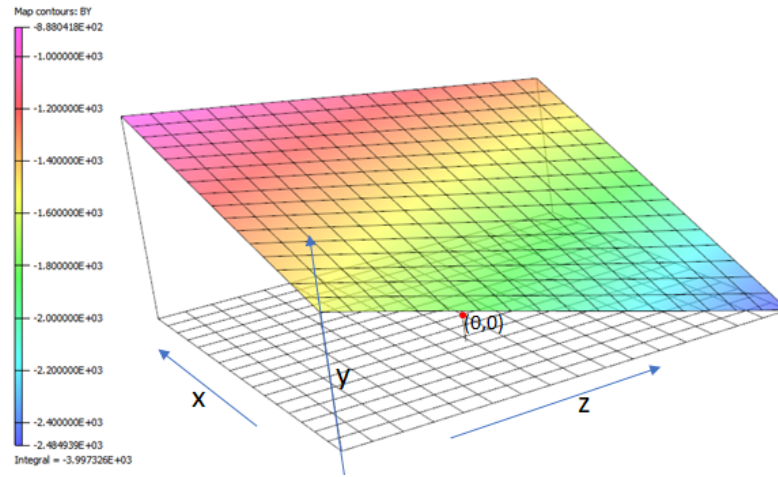


Figure 6: A histogram of the $B_y(x, y = 0, z)$ field component over the reference plane located at $y=0$. The algorithm uses the field components at the grid points shown over the rectangular area to calculate the required partial derivatives of the field components. The (0,0) point shown in the figure is the origin of the local coordinate system (x_l, y_l) for this particular "small grid area".

Results from the comparison of the "fit a function method" with the "numerical method"

The off-plane field components $[B_x(x, y_{const}, z), B_y(x, y_{const}, z), B_z(x, y_{const}, z)]$ have been calculated on four plane grids $12 \times 12 \text{ mm}^2$ and each plane has been chosen at distances $y_{const} = (0.5, 1.0, 1.5 \text{ and } 2.0)$ cm from the median plane.

Fig. 7 plots the difference of the calculated by the algorithm $B_z(\text{calc})$ component, from the "ideal" $B_z(\text{ideal})$ component as calculated by the OPERA computer method on a plane with $y=0.5$ cm.

The two plots on top in Fig. 7 correspond to the difference of the fields $[B_z(\text{calc}) - B_z(\text{ideal})]$ where $B_z(\text{ideal})$ is the field calculated by the OPERA computer code and $B_z(\text{calc})$ is the field calculated by either the "fit a function method" (left plot) or the "numerical method" (right plot). The two plots on the bottom correspond to the percent difference $100.0[B_z(\text{calc}) - B_z(\text{ideal})/B_z(\text{ideal})]$ of these fields.

In this particular example the maximum deviation of the $B_z(\text{calc})$ component from the ideal $B_z(\text{ideal})$ field is from $(-0.35 \text{ to } 0.15)$ Gauss and $(0.0 \text{ to } 0.03)$ Gauss for the "fit a function method" and the "numerical method" respectively. The percent variation of $B_z(\text{calc})$ component from the ideal $B_z(\text{ideal})$ field is from $(-0.06\% \text{ to } 0.12\%)$ and $(-0.01\% \text{ to } -0.001\%)$ for the "fit a function method" and the "numerical method" respectively.

The following Figs. 8, 9, and 10 are similar to Fig. 7 but the fields have been calculated at plane with y coordinate (1.0, 1.5, and 2.0) cm.

Both methods the "fit a function" and the "numerical" method of calculating the off-plane field components provide accurate results with less than 1% relative error when the field component are calculated at a y-distance < 2.0 cm from the reference plane ($y=0$). It is understood that this 2.0 cm limit depends on the aperture of the magnet which in this example is 4.4 cm. In this example only the $B_z(x, y_{const}, z)$ has been chosen for comparison in the Fig. 7, 8, 9, and 10 because for

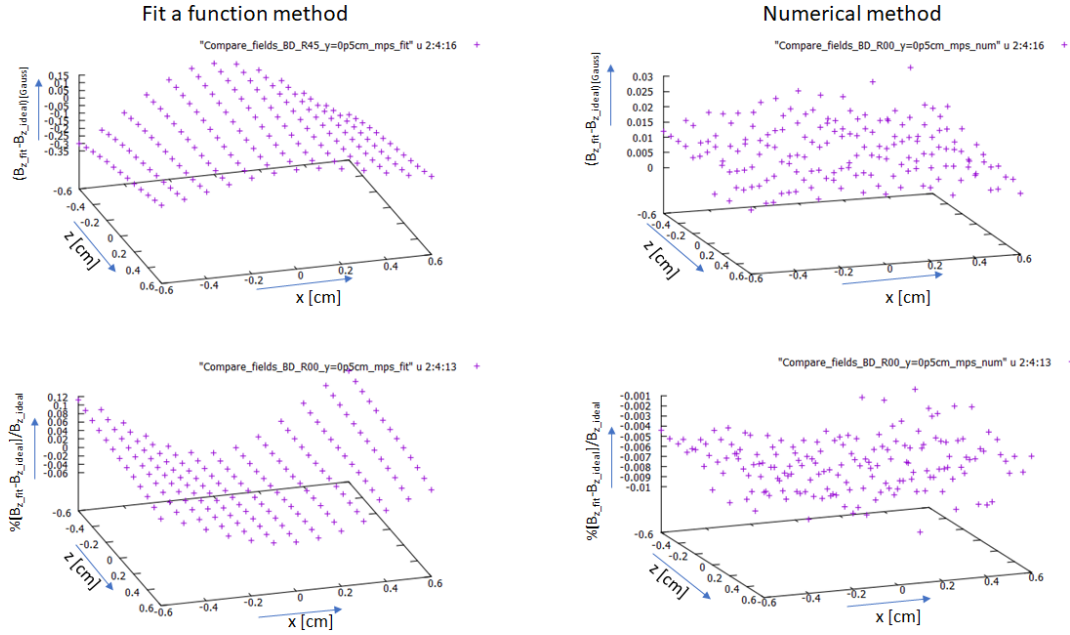


Figure 7: The two plots on top correspond to the difference of the fields $[B_z(\text{calc}) - B_z(\text{ideal})]$ where the $B_z(\text{calc})$ was calculated with the "fit a function method" (left plot) and the "numerical method" (right plot). The two plots on the bottom correspond to the percent difference $100.0[B_z(\text{calc}) - B_z(\text{ideal}) / B_z(\text{ideal})]$.

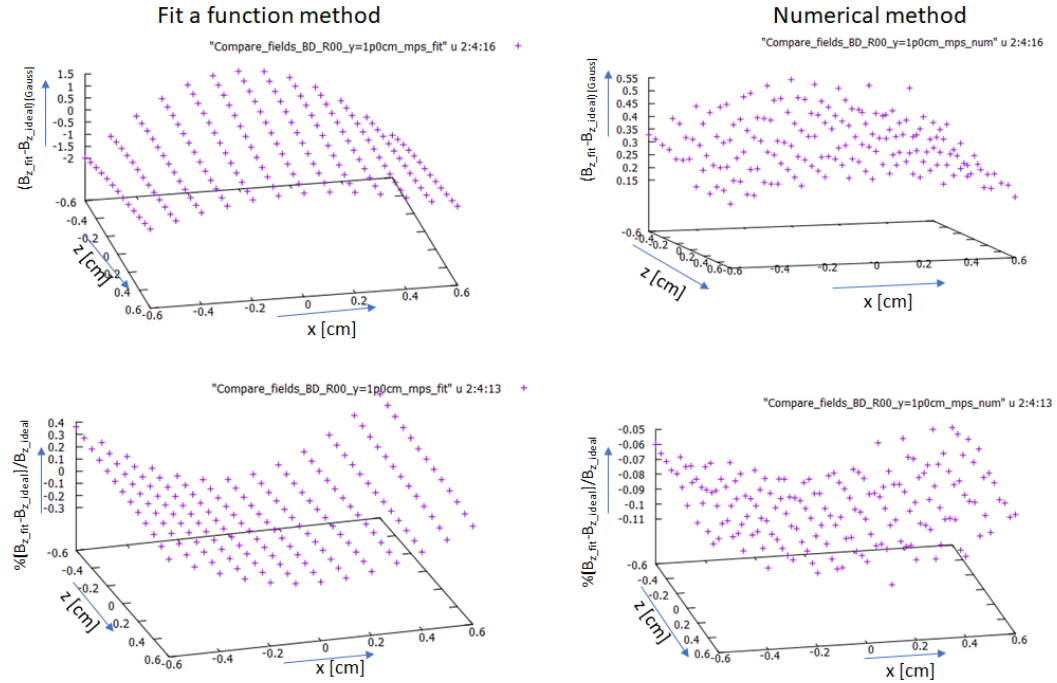


Figure 8: Same as Fig. 7 but the plane the field are calculated are at $y=1.0$ cm from the reference plane ($y=0.0$).

some reason it yields a bit higher error as compared with the other two components $B_x(x, y_{const}, z)$, and $B_y(x, y_{const}, z)$. As was demonstrated earlier both methods depend on the partial derivatives of the field components on the plane where the fields are measured and these partial derivatives of the field components as calculated by the "fit a function method" and the "numerical method" appear in Table 1 of APPENDIX I.

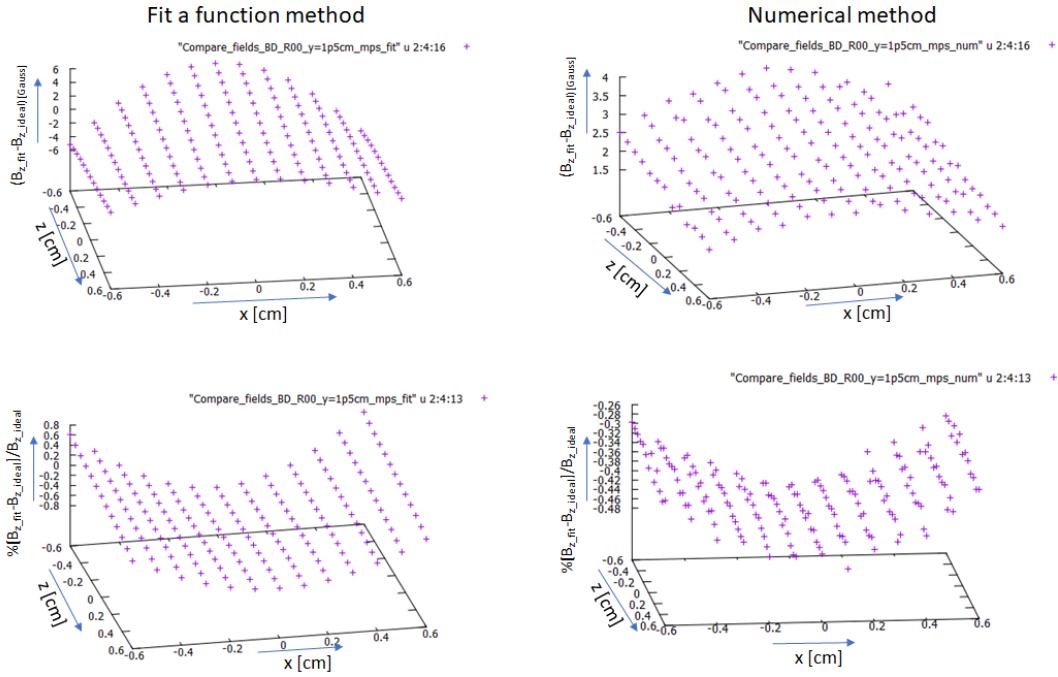


Figure 9: Same as Fig. 7 but the plane the field are calculated are at $y=1.5$ cm from the reference plane.

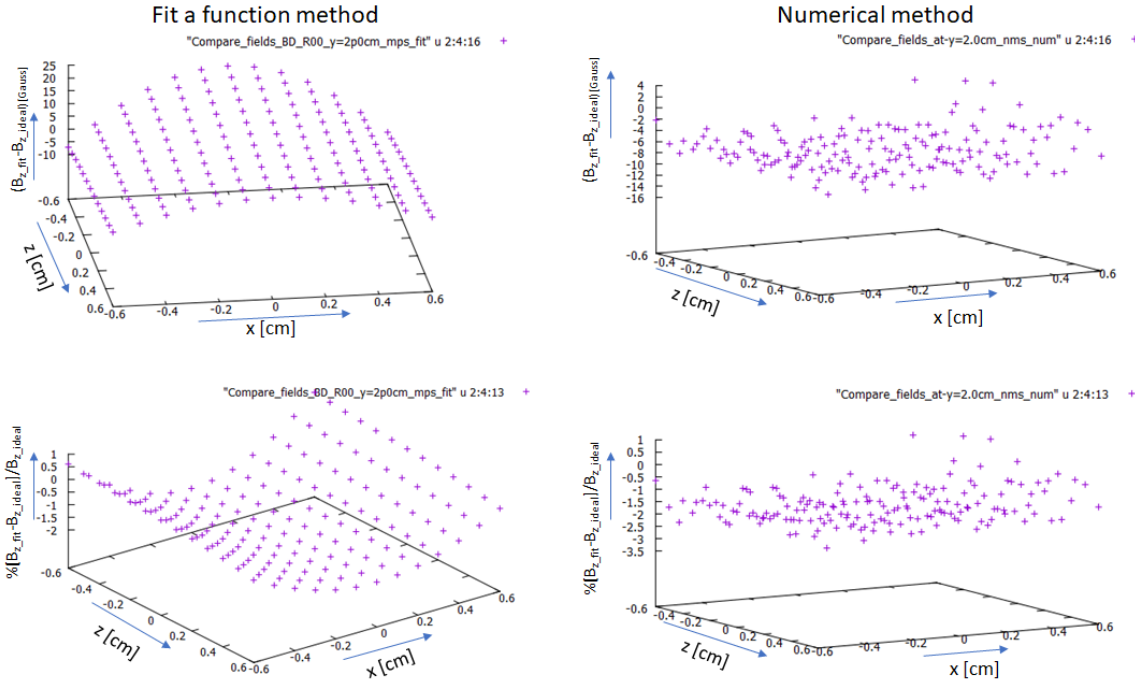


Figure 10: Same as Fig. 7 but the plane the field are calculated are at $y=2.0$ cm from the reference plane.

COMPARISON OF THE "fit a function method" WITH THE "numerical method" NON MEDIAN PLANE SYMMETRY

This section is similar to the previous one but it is related to the calculation of off-plane field components from the knowledge of the field components on a plane grid which is not a symmetry plane of the magnet. A way to generate a non symmetry plane is to rotate the magnet shown in Fig. 5 by some angle about the longitudinal z -axis. Fig. 11 is an isometric view of such a magnet rotated by 45° angle about the z -axis. As in the case of the magnet with median plane symmetry, a small rectangular area $16 \times 16 \text{ mm}^2$ has been chosen on the x, z plane at $y=0$ and the field component $[B_x(x, y = 0, z), B_y(x, y = 0, z), B_z(x, y = 0, z)]$ have been recorded on a rectangular grid with spacing 1 mm in either x or

z direction. The colors on the $16 \times 16 \text{ mm}^2$ small area shown in Fig. 11 are the contours of the $B_x(x, y = 0, z)$ component which has been calculated using the 3D OPERA computer code. A histogram plot of the $B_x(x, y = 0, z)$ component over this rectangular area is shown in Fig. 12. The same procedure which was used in the previous section to calculate the off-plane field components $[B_x(x, y_{const}, z), B_y(x, y_{const}, z), B_z(x, y_{const}, z)]$ from the known components on the plane grid with median plane symmetry, is also used in this section.

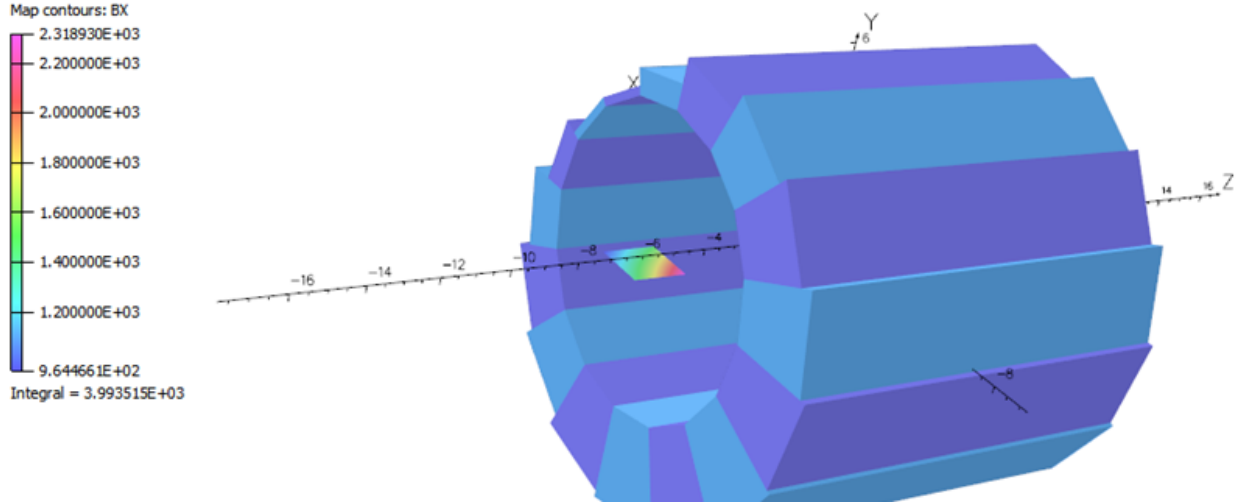


Figure 11: An isometric view of the magnet with no symmetry plane. This magnet is identical to the magnet shown in Fig. 5, but rotated by 45° about the z-axis. In OPERA code rotating the permanent magnets by an angle does rotate the magnetization vector of each permanent magnet therefore the field of the rotated magnet is not related to the field of the non-rotated magnet. This is not a issue since the goal is to generate a magnet which does not possess a symmetry plane.

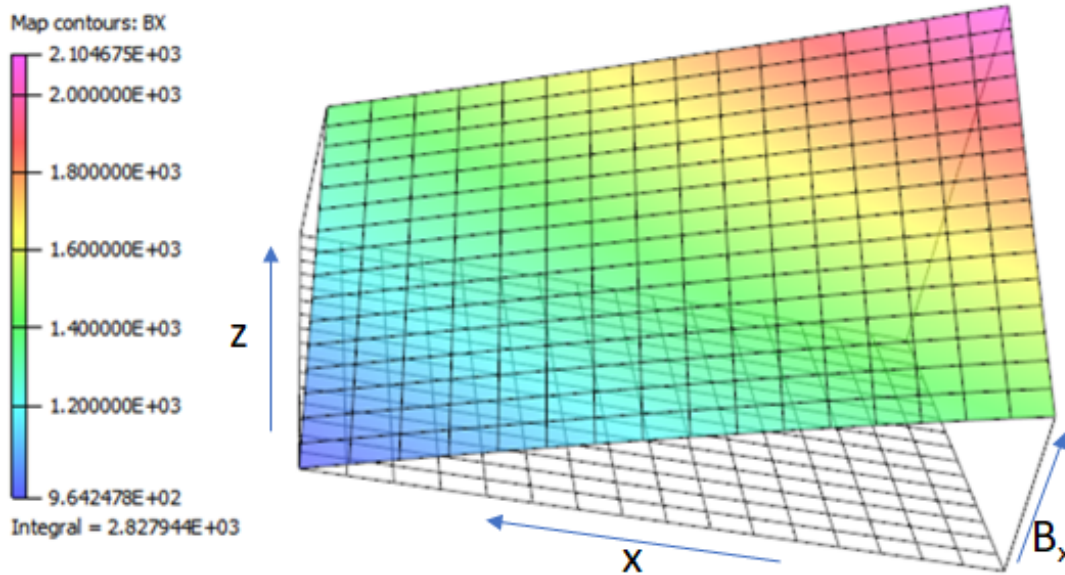


Figure 12: A histogram plot of the $(B_x(x, y = 0, z))$ component over the small area of $18 \times 18 \text{ mm}^2$. The $(B_x(x, y = 0, z))$ component has been calculated by the 3D OPERA computer code. Only the values of the components on the grid points are used by the two methods discussed in this paper.

Results from the comparison of the "fit a function method" with the "numerical method"

The off-plane field components $[B_x(x, y_{const}, z), B_y(x, y_{const}, z), B_z(x, y_{const}, z)]$ have been calculated on plane grids $12 \times 12 \text{ mm}^2$ in area. Four planes has been selected at distances $y_{const} = (0.5, 1.0, 1.5 \text{ and } 2.0) \text{ cm}$ from the reference plane

respectively. The 3D plots in Figs 13, 14, 15, and 16, are similar to Fig. 7, 8, 9, and 10 but they correspond to the fields of a reference plane which does not possess median plane symmetry. Table 2 in APPENDIX I tabulates these partial derivatives of the field components as calculated by the "fit a function method" and the "numerical method" for comparison.

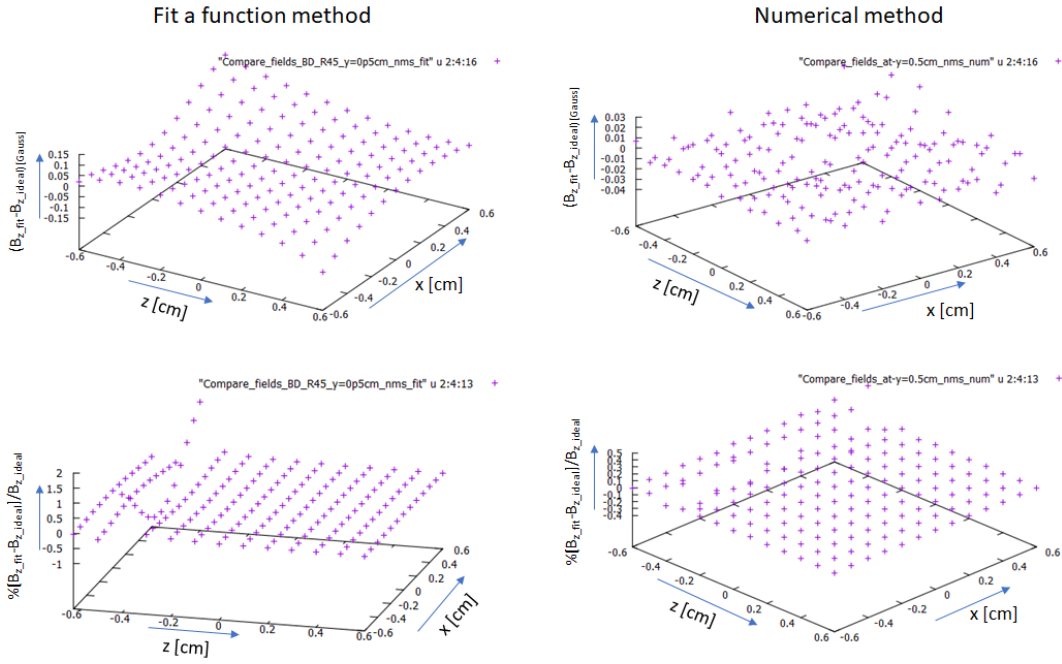


Figure 13: Same as Fig. 7 but the reference plane is not a symmetry plane.

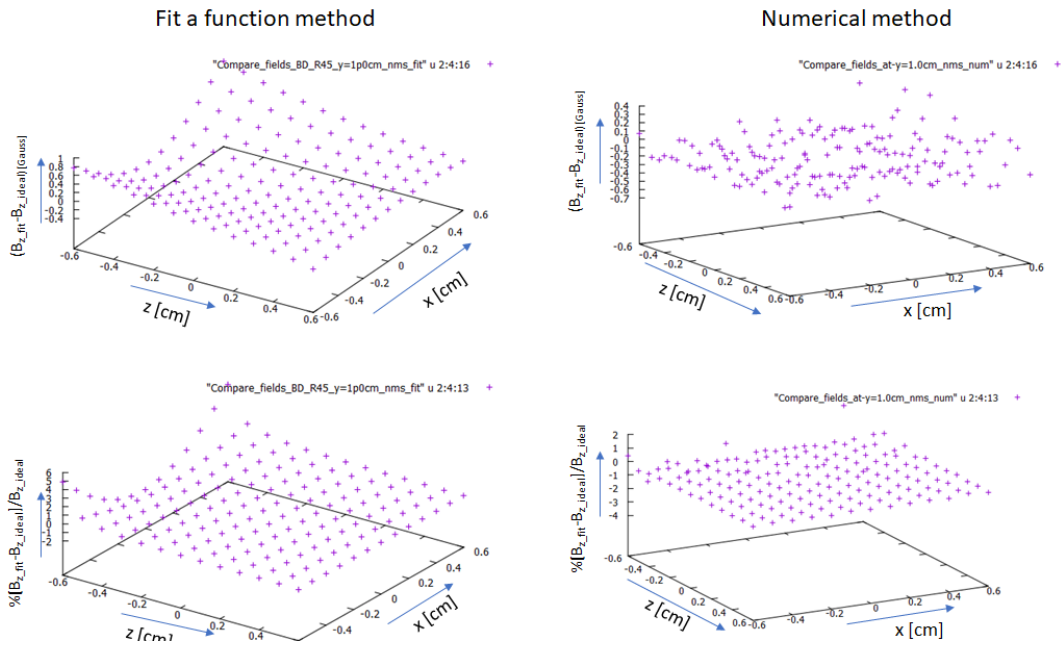


Figure 14: Same as Fig. 13 but the plane the field are calculated are at $y=1.0$ cm from the reference plane.

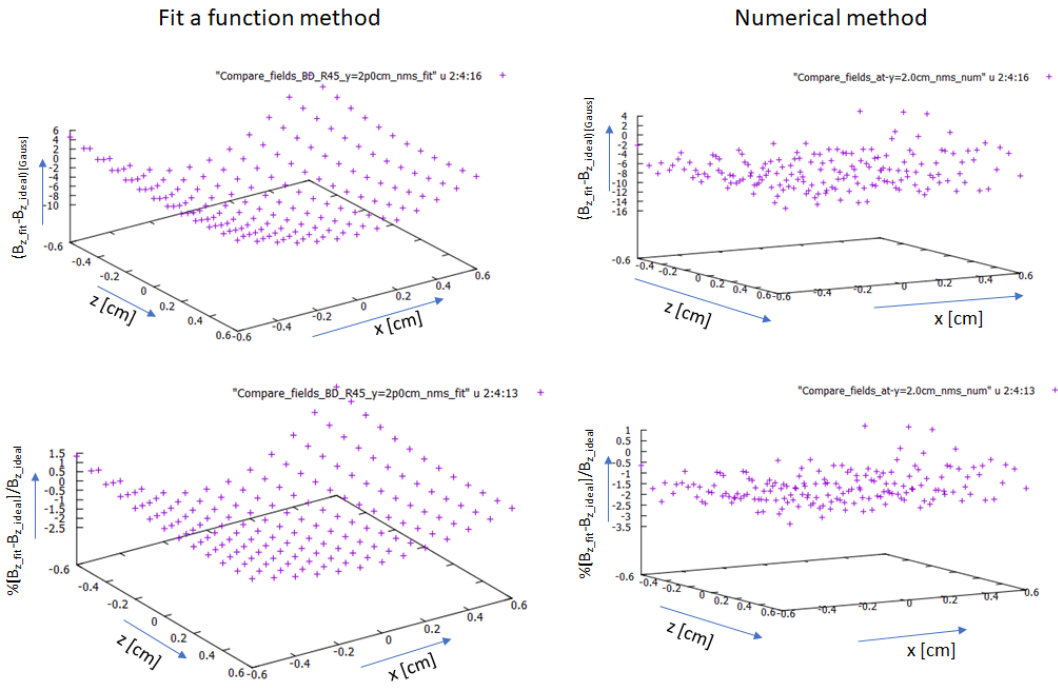


Figure 15: Same as Fig. 13 but the plane the field are calculated are at $y=1.5$ cm from the reference plane.

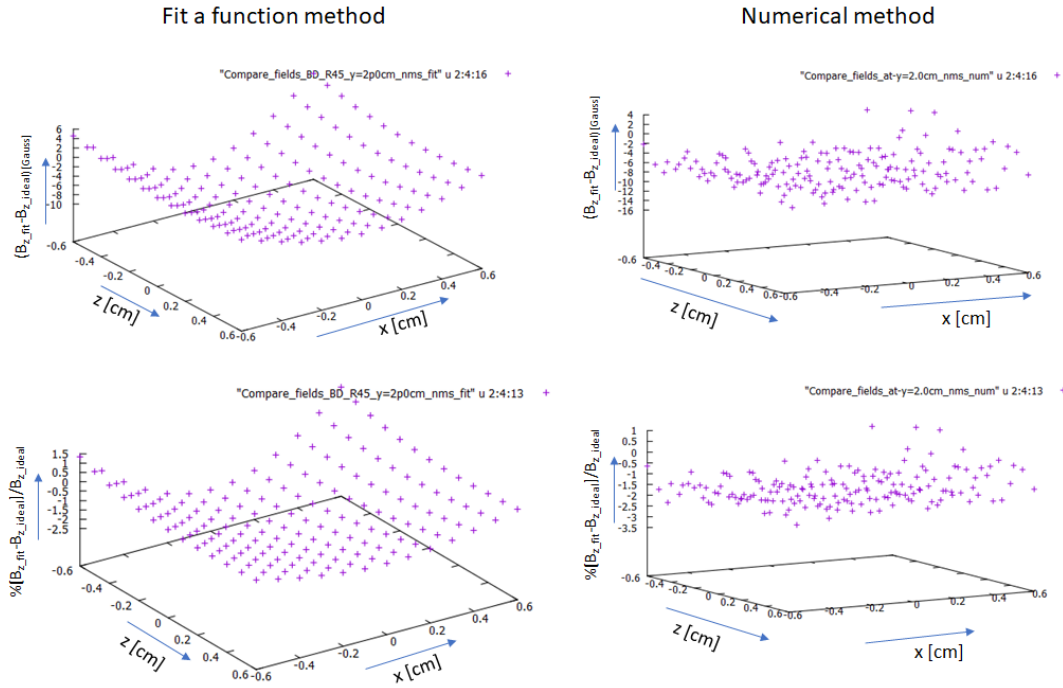


Figure 16: Same as Fig. 13 but the plane the field are calculated are at $y=2.0$ cm from the reference plane.

CONCLUSION

The algorithm to calculate the $[B_x(x, y, z), B_y(x, y, z), B_z(x, y, z)]$ field components of the magnetic field at a point (x, y, z) in space, from the knowledge of the components $[B_x(x, y = 0, z), B_y(x, y = 0, z), B_z(x, y = 0, z)]$ on a plane normal to the y -axis at $y=0$ has been applied on two magnets, each having an aperture of 4.4 cm. One of the magnets possess median

plane symmetry and the other with no median plane symmetry. The off-plane median plane field components calculated using this algorithm yield relative error of less than 1% for field points at distances less than 2 cm from the reference plane where the field components are measured on a rectangular grid of the plane. The required spatial partial derivatives of the field components $[B_x(x, y = 0, z), B_y(x, y = 0, z), B_z(x, y = 0, z)]$ were calculated using the "fit a function" method and the "numerical" method. No significant difference is observed using either of the methods to calculate the partial derivatives. The use of "fit a function" method provides the derivatives at the point where the particle is located therefore it provides the required fields at the location of the particle as needed. The fit a function method may also work as a "smoothing" of the values of the experimentally measured field components. However this method requires the partition of the 2D field map in smaller-grid-planes for the polynomial function to fit with accuracy the experimental points.

The use of the "numerical" method provides the derivatives at the grid points (x_{grid}, z_{grid}) where the fields on the plane are measured therefore it may provide better accuracy than the "fit a function" method. However to calculate the field components at the particle location (x, y, z) other than a grid point, the field components at four adjacent grid points (x_{grid}, y, z_{grid}) should be calculated and the field components at required point (x, y, z) can be obtained by linear interpolation of the calculated field components at these four grid points. The error of measuring the field components on the 2D grid determines the degree of accuracy of the off-plane calculated fields. Such an error study is planned to be carried out in another paper.

APPENDIX I

For a magnet with median plane symmetry $[B_x(x, y = 0, z) = 0, B_y(x, y = 0, z), B_z(x, y = 0, z) = 0]$ Table 1 lists the partial derivatives of the field components on the reference plane as calculated by the "fit a function" method and "numerical" method up to 4th order. Only the partial derivatives at the point with coordinates $(x_l, z_l) = (0.0, 0.0)$ of the local coordinate system are listed.

For a magnet with no median plane symmetry $[B_x(x, y = 0, z), B_y(x, y = 0, z), B_z(x, y = 0, z)]$ Table 2 lists the partial derivatives of the field components on the reference plane as calculated by the "fit a function" method and "numerical" method up to 4th order. Only the partial derivatives at the point with coordinates $(x_l, z_l) = (0.0, 0.0)$ of the local coordinate system are listed. From the values of the derivatives up to third order appearing in Table 1 there is agreement between the two methods. There is some disagreement between the 4th order derivative of the two methods and this is under investigation.

REFERENCES

- [1] Ref. of the et. al. "The CBETA project: arXiv.org > physics > arXiv:1706.04245"
- [2] S.B. Kowalski and H.A. Enge "The Ion-Optical Program Raytrace" NIM A258 (1987) 407
- [3] N. Tsoupas et. al. "Effects of Dipole Magnet Inhomogeneity on the Beam Ellipsoid" NIM A258 (1987) 421-425
- [4] Zgoubi computer code
- [5] F. Lemuet, F. Meot, Developments in the ray-tracing code Zgoubi for 6-D multiturn tracking in FFAG rings, Nuclear Instruments and Methods in Physics Research A 547 (2005) 638–651
- [6] J. Fourier, F. Martinache, F. Meot, J. Pasternak Spiral FFAG lattice design tools. Application to 6-D tracking in a proton-therapy class lattice Nuclear Instruments and Methods in Physics Research A 547 (2005) 638–651

Table 1: Calculated derivatives at local coordinates $(x_l, z_l) \Rightarrow (0.0, 0.0)$. The reference plane is a symmetry plane.

Order	Method	$B_x(x, 0, z)$	$B_y(x, 0, z)$	$B_z(x, 0, z)$						
0^{th}										
	function	0.000	-1572.011	0.000						
	numeric	0.000	-1572.011	0.000						
1^{st}		$\frac{\partial B_x(x, z)}{\partial x}$	$\frac{\partial B_y(x, z)}{\partial x}$	$\frac{\partial B_y(x, z)}{\partial z}$	$\frac{\partial B_z(x, z)}{\partial z}$					
	function	0.00000	570.09231	-431.90261	0.00000					
	numeric	0.00000	570.09256	-431.96004	0.00000					
2^{nd}		$\frac{\partial^2 B_x(x, 0, z)}{\partial x^2}$	$\frac{\partial^2 B_x(x, 0, z)}{\partial x \partial z}$	$\frac{\partial^2 B_y(x, 0, z)}{\partial x^2}$	$\frac{\partial^2 B_y(x, 0, z)}{\partial z^2}$	$\frac{\partial^2 B_z(x, 0, z)}{\partial x \partial z}$	$\frac{\partial^2 B_z(x, 0, z)}{\partial z^2}$			
	function	0.00000	0.00000	-0.52016	2.14901	0.00000	0.00000			
	numeric	0.00000	0.00000	-0.51066	2.14844	0.00000	0.00000			
3^{rd}		$\frac{\partial^3 B_x(x, 0, z)}{\partial x^3}$	$\frac{\partial^3 B_x(x, 0, z)}{\partial x \partial z^2}$	$\frac{\partial^3 B_y(x, 0, z)}{\partial x^3}$	$\frac{\partial^3 B_y(x, 0, z)}{\partial x^2 \partial z}$	$\frac{\partial^3 B_y(x, 0, z)}{\partial x \partial z^2}$	$\frac{\partial^3 B_y(x, 0, z)}{\partial z^3}$	$\frac{\partial^3 B_z(x, 0, z)}{\partial x^2 \partial z}$	$\frac{\partial^3 B_z(x, 0, z)}{\partial z^3}$	
	function	0.00000	0.00000	0.18314	-16.84934	-0.38131	76.00816	0.00000	0.00000	
	numeric	0.00000	0.00000	0.12207	-16.90674	-0.42725	78.12500	0.00000	0.00000	
4^{th}		$\frac{\partial^4 B_x(x, 0, z)}{\partial x^4}$	$\frac{\partial^4 B_x(x, 0, z)}{\partial x^3 \partial z}$	$\frac{\partial^4 B_x(x, 0, z)}{\partial x^2 \partial z^2}$	$\frac{\partial^4 B_x(x, 0, z)}{\partial x \partial z^3}$	$\frac{\partial^4 B_y(x, 0, z)}{\partial x^4}$	$\frac{\partial^4 B_y(x, 0, z)}{\partial x^2 \partial z^2}$	$\frac{\partial^4 B_y(x, 0, z)}{\partial z^4}$	$\frac{\partial^4 B_z(x, 0, z)}{\partial x^3 \partial z}$	$\frac{\partial^4 B_z(x, 0, z)}{\partial x^2 \partial z^2}$
	function	0.00000	0.00000	0.00000	0.00000	-0.01799	0.07320	0.07916	0.00000	0.00000
	numeric	0.00000	0.00000	0.00000	0.00000	-2.44141	-1.22070	0.00000	0.00000	0.00000
4^{th}		$\frac{\partial^4 B_z(x, 0, z)}{\partial x} \partial z^3$	$\frac{\partial^4 B_z(x, 0, z)}{\partial z^4}$							
	function	0.00000	0.00000							
	numeric	0.00000	0.00000							

[7] Stephen Brooks Off-Axis Magnetic Fields Extrapolated from On-Axis Multipoles <http://stephenbrooks.org/ap/report/2013-10/offaxis.pdf>

[8] H.A. Enge, Deflecting Magnets, in “Focusing of Charged. Particles”, edited by A. Septier, Academic Press, 1967

[9] Numerical Recipes. The Art of Scientific Computing. page 58

[10] N. Tsoupas et. al. “Closed Orbit Calculations at AGS and Extraction Beam Parameters at H13” AD/RHIC/RD-75

[11] Vector Field Inc. <https://www.manta.com/c/mmmnm9hz/vector-fields-incorporated>

